Roman coins at the edge of the Negev: characterisation of copper alloy artefacts and soil from Rakafot 54 (Beer Sheva, Israel)

ACTA IMEKO
ISSN: 2221-870X
December 2022, Volume 11, Number 4, 1 - 6

Roman coins at the edge of the Negev: characterisation of copper alloy artefacts and soil from Rakafot 54 (Beer Sheva, Israel)

Manuel J. H. Peters[1,2], Yuval Goren[3], Peter Fabian[3], José Mirão[4,5], Carlo Bottaini[4], Sabrina Grassini[1], Emma Angelini[1]

[1] *Department of Applied Science and Technology, Politecnico di Torino, Corso Duca degli Abruzzi 24, 10129 Torino, Italy*
[2] *Department of History, Universidade de Évora, Largo dos Colegiais 2, 7000-803 Évora, Portugal*
[3] *Department of Bible, Archaeology & Ancient Near East, Ben-Gurion University of the Negev, Israel*
[4] *HERCULES Laboratory, Institute for Advanced Studies and Research, University of Évora, Largo Marquês de Marialva 8, 7000-809 Évora, Portugal*
[5] *Geosciences Department, School of Sciences and Technology, University of Évora, Rua Romão Ramalho 59, 7000-671, Évora, Portugal*

ABSTRACT
The research presented in this paper focused on the preliminary non- and semi-destructive analysis of copper alloys, corrosion, and soil components from a Roman archaeological site in Israel. Investigations using portable X-ray fluorescence, X-ray diffraction and scanning electron microscopy with energy dispersive spectroscopy as well as micromorphological analyses were carried out to gain a better understanding of the corrosion processes affecting the copper alloy artefacts, by characterising the alloy composition, soil environments, and corrosion products. Preliminary results indicate that the artefacts consist of copper-lead-tin alloys, covered by copper hydroxy-chlorides and lead sulphate phases with slight variations in their crystallisation. The multi-analytical approach revealed the presence of quartz, calcite, gypsum and feldspars in the sediments, while thin sections more specifically indicate loess soils with local micro-environments.

Section: RESEARCH PAPER

Keywords: Archaeometry; archaeometallurgy; archaeological materials science; classical archaeology; Near Eastern archaeology

Citation: Manuel J. H. Peters, Yuval Goren, Peter Fabian, José Mirão, Carlo Bottaini, Sabrina Grassini, Emma Angelini, Roman coins at the edge of the Negev: characterisation of copper alloy artefacts and soil from Rakafot 54 (Beer Sheva, Israel), Acta IMEKO, vol. 11, no. 4, article 13, December 2022, identifier: IMEKO-ACTA-11 (2022)-04-13

Section Editor: Tatjana Tomic, Industrija nafte Zagreb, Croatia

Received April 26, 2022; **In final form** December 14, 2022; **Published** December 2022

Corresponding author: Manuel J. H. Peters, e-mail: manueljhpeters@gmail.com

1. INTRODUCTION

This research discusses the analysis of several copper alloy artefacts from an arid site on the edge of the Negev desert in Israel. Rakafot 54 was excavated during two seasons in 2018 and 2019 as a collaboration between the Israel Antiquities Authority and Ben-Gurion University of the Negev (Figure 1). The site was probably established during the first century CE and demolished during the Bar Kochba revolt against Rome (132-135/6 CE) [1]. Several indications of regular habitation have been found, including oil lamp fragments and limestone vessels. The site is placed near the border between Judea and Nabataea, close to a Roman road, and includes a watchtower, hearths, garbage pits, and an underground system. Numerous artefacts were found during the two seasons of excavation, including various imperial and provincial Roman copper alloy coins. This includes copper alloy coins minted by Herod Agrippa I (ruled 41-44 CE) and the Roman procurators in Judaea (6-66 CE). Additionally, provincial Roman coins minted in Ashkelon during the reign of Nero to Trajan (37-117 CE), Nabataean coins (until 106 CE) and coins of the First Jewish–Roman War (66–73 CE) were found.

In terms of the geological setting, the site is located on quaternary alluvium loess soil. The loess is soft yellow windblown silty sediment, dominated by quartz silt, clay and calcite. The loess deposition, by southern-western winds from Sinai and North Africa, started at the end of the Pleistocene and continues into the Holocene. The formation is bordered to the

west and the south by a coastline of calcareous sandstone and sand dunes, to the east by the Eocene Adulam formation which is mainly chalk and chert, and to the north by quaternary red sand and loam (locally termed Hamra soil) [2]. In the Beer Sheva area, where mean annual precipitation is 200–350 mm, loess covers the entire landscape and pre-existing topography [3]. The soil components of the archaeological site are largely dependent on this general geological setting, with local variations due to anthropogenic activities and post-depositional processes. These variations could possibly lead to micro-environments corresponding to the various excavation loci.

The copper alloy objects coming from the site were covered with a heterogeneous layer of corrosion products and sediment (Figure 2). The items were retrieved from different areas, which contained sediments that appeared to have distinctively different compositions, based on a visual inspection. This could possibly affect the corrosion process in various ways. In order to gain a better understanding of both the degradation processes affecting these artefacts and to determine their state of preservation and possible future steps for conservation, a selection of artefacts was analysed with portable X-ray fluorescence (pXRF), X-ray diffraction (XRD), and scanning electron microscopy with energy dispersive spectroscopy (SEM-EDS). The reason behind this approach lies in the general need to avoid intrusive sampling of museum objects and the requirement for the exclusive application of non-destructive testing (NDT) techniques for the material characterisation of cultural artefacts. As a result, research is gradually becoming reliant on portable instrumentation (e.g. pXRF) that is intended to screen only the surfaces of the objects under investigation. However, especially in the case of metals, the effects of chemical-physical processes responsible for degradation and corrosion as well as surface enrichment or loss of elements make NDT highly problematic. Metallic objects can be covered in thick layers consisting of corrosion products and soil components, which usually means that surface analysis to investigate alloy components of the bulk material becomes relatively inaccurate. If it is possible to expose a small area of the bulk material below the corrosion layers, SEM-EDS can be carried out to validate the results obtained with pXRF. Although the degradation processes of metallic artefacts are well-known and widely investigated, every artefact has a specific history strictly related to its depositional micro-environment [4]. The environmental parameters influence the corrosion process and affect the various areas of the metallic objects differently. Consequently, it is of high importance to assess the specific deterioration of the artefacts in order to be able to interpret the results of NDT surface investigation.

Figure 2. Copper alloy coin with corrosion and soil.

In this paper, several artefacts and soil samples that have a clear connection were considered. The main goal of this research was to gain information on the elemental composition of the coins, as well as identifying the corrosion products, and assessing the soil components. This was done by using a multi-analytical methodology involving elemental and mineralogical characterisation, as well as microscopy. The bulk of this research was performed at Ben-Gurion University of the Negev.

2. MATERIALS AND METHODS

This research investigated the alloys, corrosion products, and related soil of a group of corroded metallic coins from Rakafot 54. During the excavation, the location of the metallic artefacts was recorded by assigning them to the specific locus they originated from, and the same was done for the soil samples. For this research, six coins and their related soil samples were selected.

A preliminary pXRF surface screening was carried out on the coins prior to conservation treatment, to determine the major alloy components of the coins. A Thermo Scientific Niton XL3t GOLDD+ XRF Analyser equipped with a Geometrically Optimized Large Area Drift Detector and 50 kV, 200 μA Ag anode was used, with an 8 mm collimator. The data was obtained with the Cu/Zn mining measurement mode, with a duration of 120 seconds. Both sides of each coin were measured.

XRD measurements were performed separately on the corrosion samples collected from the artefacts. Sampling was done by carefully removing some milligrams of corrosion from the objects with a scalpel, paying attention to not damage the limitos (the surface boundary between the external corrosion products and the corrosion that has replaced the bulk metal,

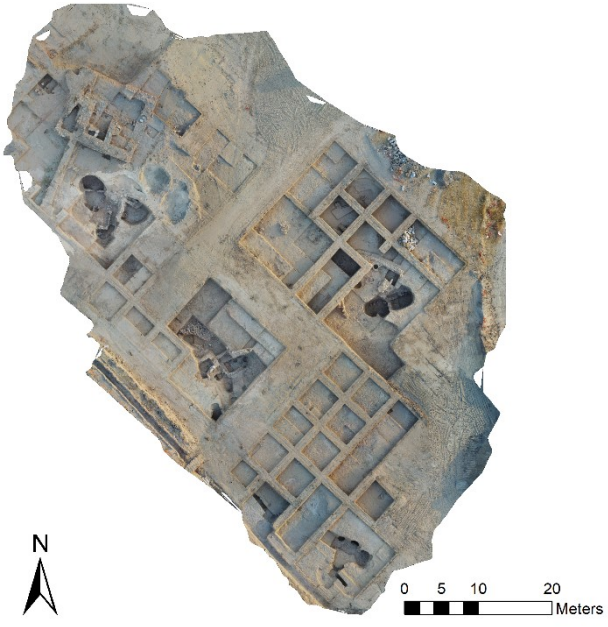

Figure 1. Aerial orthophoto of the archaeological site of Rakafot 54.

Table 1. Sample types and analytical techniques.

Sample type	Technique	Information
Artefact surface	pXRF	Alloy & soil
Exposed bulk material	SEM-EDS	Alloy & microstructure
Corrosion powder	XRD	Corrosion & soil
Soil thin section	Petrography	Soil

Table 2. Primary alloy components (wt%) on artefact surface, obverse (a) and reverse (b).

Sample	Cu	Pb	Sn	Zn	Ag
B6058a	46.8	5.1	2.7	0.04	< 0.03
B6058b	45.1	5.7	1.0	< 0.03	< 0.03
B6081a	44.6	13.0	3.4	< 0.05	< 0.04
B6081b	47.5	5.6	0.45	< 0.03	< 0.03
B6101a	42.1	6.8	1.5	< 0.04	< 0.03
B6101b	36.0	14.4	4.4	< 0.04	< 0.04
B8103a	43.0	1.1	0.04	< 0.04	< 0.02
B8103b	36.0	3.4	2.1	0.02	< 0.02
B8764a	43.9	3.2	0.34	0.03	< 0.02
B8764b	46.5	3.0	2.6	0.05	< 0.03
B9803a	44.0	5.1	1.3	< 0.03	< 0.02
B9803b	32.1	14	5.0	< 0.04	< 0.04

Table 4. Trace elements (wt%) on artefact surface, obverse (a) and reverse (b).

Sample	Mg	Mn	Ni	P	Ti
B6058a	< 2.4	< 0.02	0.02	0.11	0.11
B6058b	< 3.4	< 0.03	0.02	0.16	0.17
B6081a	< 2.6	< 0.02	0.04	0.80	0.04
B6081b	< 3.1	< 0.02	0.01	0.07	0.05
B6101a	2.6	< 0.03	< 0.02	0.29	0.13
B6101b	2.9	0.02	0.01	0.60	0.06
B8103a	< 4.0	< 0.02	< 0.02	0.31	0.11
B8103b	< 4.4	< 0.02	< 0.02	0.46	0.17
B8764a	< 4.0	< 0.02	0.03	0.29	0.12
B8764b	< 4.4	< 0.02	0.02	0.08	0.09
B9803a	< 2.4	< 0.03	< 0.02	0.14	0.12
B9803b	< 2.0	0.03	0.02	0.28	0.23

isomorphic with the uncorroded artefact). The samples were then homogenised by grinding them, using an agate mortar and a few drops of ethanol. This emulsion was positioned in the middle of a zero-background silicon sample holder and flattened, after which the ethanol was left to evaporate. Diffractograms were taken from the samples with a PANalytical X'Pert Pro powder X-ray diffractometer equipped with PIXcel 1D detector and a Cu K-alpha source with wavelength 1.54 Å, at 40 kV with a current of 40 mA.

Thin sections from the soil samples were obtained by embedding a portion of each sample in epoxy resin, mounting it on a glass microscope slide, and grinding and polishing it to 30 μm. The thin sections were then observed with a petrographic microscope under polarised light. SEM-EDS was carried out on a small exposed area of the bulk metal of the artefacts, using a Micro FASEM FEI Quanta 200 scanning electron microscope under high vacuum at 25.00 kV.

An overview of the sample types, analytical techniques and the expected information can be found in Table 1.

3. RESULTS

3.1. pXRF

The preliminary pXRF screening of the coins indicated that the coins are made of copper-lead-tin alloys, with relatively high amounts of lead in some cases (Table 2). The presence of silver is below the limit of detection, and zinc appears to be only present as trace element in some cases. There are inconsistencies between the measurements on the obverse (a) and reverse (b) sides of each coin, probably stemming from the position of the samples on the instrument, and the fact that these measurements were carried out on uncleaned objects. Consequently, the results are largely dependent on the corrosion layers and sediments present on the surface. Nevertheless, these results offer a useful indication of the primary alloy components of the coins found at the site and offer a clue of the possible corrosion products.

Table 3. Soil components (wt%) on artefact surface, obverse (a) and reverse (b).

Sample	Al	Ca	Cl	Fe	K	S	Si
B6058a	2.1	8.7	4.61	0.51	0.25	1.12	9.1
B6058b	2.3	4.9	5.09	0.81	0.38	1.52	13.1
B6081a	1.4	5.4	5.77	0.13	0.11	3.81	4.7
B6081b	0.9	2.9	9.9	0.34	0.15	2.18	3.2
B6101a	2.1	6.0	5.46	0.68	0.35	2.20	9.1
B6101b	1.0	10.1	3.22	0.33	0.20	3.44	9.1
B8103a	1.9	7.4	3.67	0.59	0.31	0.55	11.9
B8103b	1.6	8.4	1.27	0.77	0.34	1.42	13.4
B8764a	1.9	4.9	8.0	0.60	0.32	1.66	7.4
B8764b	1.7	10.6	6.27	0.51	0.26	1.33	6.0
B9803a	2.7	10.7	4.33	0.56	0.39	1.13	11.5
B9803b	3.2	13.9	2.34	1.25	0.70	1.35	12.5

Additionally, the pXRF measurements provide information about the traces of sediments that are possibly present on the surface of the artefacts together with the formed corrosion phases (Table 3). Significant amounts of calcium, chlorine and silicon can be observed as well as smaller amounts of aluminium, potassium, and sulphur. Additional components can be found in Table 4.

3.2. Petrography

The thin sections of all the soil samples observed under the petrographic microscope revealed a matrix that is silty and highly calcareous. The silt is well-sorted and contains mainly quartz, but also a recognisable quantity of other minerals, including hornblende, zircon, mica minerals, feldspars, tourmaline, augite and more rarely garnet, epidote and rutile. Ore minerals are abundant too in this fraction. The sand fraction includes dense, well sorted, rounded sand-sized quartz grains, and limestone. Based on a bulk of published data it is readily identified as loess soil [5]. However, micromorphological features within this given theme indicate more specific micro-environments, resulting from an array of anthropogenic activities as well as post-depositional processes. The post-depositional processes are

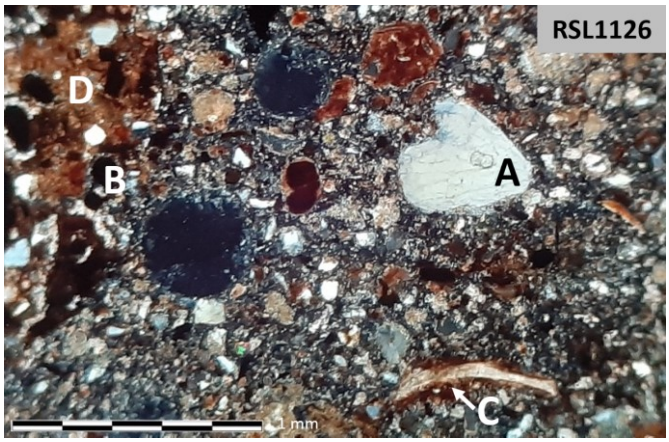

Figure 3. Petrographic image showing silty and calcareous matrix with rounded quartz sandy grain (A), charred ash material (B), shell fragment (C), and burnt soil with ferric corrosion products (D).

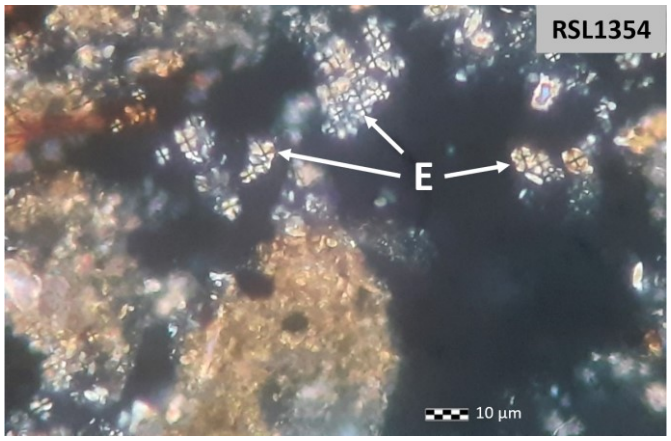

Figure 4. Petrographic image showing herbivore dung spherulites (E) in ash layer from a hearth.

reflected by re-crystallisation of calcite and gypsum from ground water, corrosion products of metals (Figure 3), mineral replacements, clay relocation, etc. Anthropogenic features include remnants of human activities such as slag, coprolites, pottery and brick crumbs, charred plant remains, phytolith concentrations, and other ash characteristics (Figure 4). All these will be used in further research to define the immediate micro-environmental physiognomies of the sediment at the immediate proximity of each artefact, in order to correlate it with the corrosion composition.

3.3. XRD

XRD diffractograms which include the representative peaks for these samples are shown in Figure 5. Although there are some visual differences in the diffractograms, mainly related to variations of peak intensities due to sample preparation, the main components appear to be relatively consistent.

The primary compound in all samples was identified as atacamite ($Cu_2(OH)_3Cl$), the orthorhombic version of copper hydroxy-chloride, which can be commonly found on copper alloy archaeological objects extracted from salty soils [6]. Clinoatacamite, its monoclinic polymorph, has been detected in two samples, while its presence is not clear in the rest of the cluster under investigation. Paratacamite ($Cu_3(Cu,Zn)(OH)_6Cl_2$), a zinc-enriched variety of the copper hydroxy-chloride series, also appeared in the majority of the diffractograms (Figure 5). Even though it is not considered a polymorph, it is still closely related to atacamite as part of its degradation process [7]. The Zn

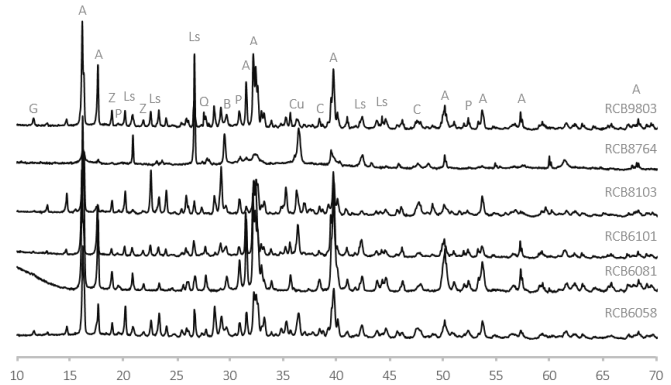

Figure 5. Diffractogram of artefact surface samples consisting of corrosion and soil minerals. A=atacamite; Cu=cuprite; Ls=lead sulphate; C=calcite; Q=quartz; G=gypsum; Z=zeolite; P=paratacamite.

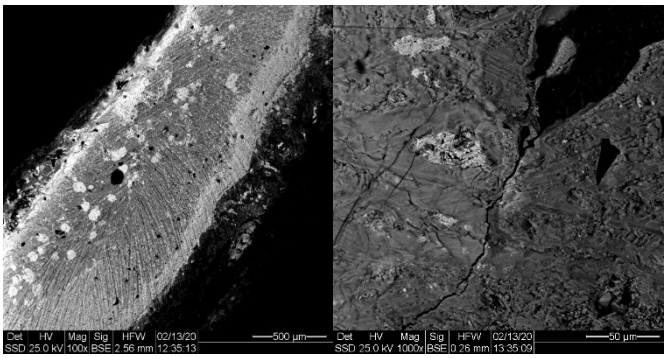

Figure 6. SEM image. Left: sample B6101 showing Cu-rich matrix with distribution of Pb globules as bright spots. Right: sample B8764 showing cavity and crack possibly improving the penetration of Cl into the bulk.

possibly originates from traces in the alloy composition. Lead sulphates were identified in most samples, while cuprite was identified in all samples except for RCB6081. This exception might be related to inconsistencies in sampling depth.

All diffractograms revealed the persistent presence of quartz, which can be explained by the traces of sediment that were present on the surface of the artefacts during the sample preparation for the XRD analyses. Other soil components that were identified in this step are K- and Na-based feldspars (albite and orthoclase), together with clay minerals such as zeolite. Gypsum and its polymorphs were identified in RCB6058, RCB6101, and RCB9803, but may also be present in other samples.

3.4. SEM

SEM-EDS results of the point analyses showed copper alloys with high amounts of lead and smaller additions of tin (Table 5). Since lead does not dissolve well in a Cu-based matrix, it usually forms globules [8]. Most of the analysed samples did indeed show a bulk matrix which is low in lead, with many lead globules distributed in the matrix, and clear cracks and crevices penetrating into the bulk in some cases (Figure 6). These cracks might aid the penetration of Cl into the bulk matrix, as shown in Table 5.

4. DISCUSSION

In order to validate the results of the individual techniques, several comparisons were made. The identification of atacamite in the diffractograms can be correlated with the presence of Cl in the pXRF results. It is still unclear whether this presence is related to the hydroxy-chloride phases of the corrosion products, or to another Cl-based mineral present in the soil. Differentiating between the lead sulphate and calcite peaks in the XRD diffractograms was complicated in some cases, however, a clear correlation could be observed between the presence of sulphur and significant amounts of lead in the pXRF data, and the presence of lead sulphate in the diffractograms. Although the presence of tin is clear in the primary alloy identification with pXRF, no tin-based corrosion products were identified in the diffractograms; however, tin oxides are reported to provide difficulties in identification with XRD [9], [10], [11]. The Si presence in the pXRF data could be related to the quartz observed in the diffractograms and the thin sections. The K and Si combination could be explained as K-based feldspars and quartz with the diffractograms, and similarly, Si and Al could be identified together in feldspars and clay minerals.

Table 5. SEM results (wt%).

Sample	Cu	Sn	Pb	Cl
B6058 bulk	67.0	1.67	27.8	3.61
B6058 Pb globule a	10.5	3.08	79.6	6.83
B6058 Pb globule b	20.4	5.56	62.2	11.8
B6058 Cu-Sn matrix	98.1	1.43	0.47	0.00
B6081 bulk a	10.9	0.44	86.3	2.33
B6081 bulk b	21.7	0.82	73.2	4.27
B6081 enriched bulk	97.2	0.00	1.80	1.02
B6101 bulk	72.6	2.90	21.1	3.33
B6101 Cu-Sn matrix	88.6	3.38	7.36	0.63
B6101 Pb globule a	12.7	0.00	69.1	18.2
B6101 Pb globule b	6.99	0.00	82.0	11.1
B8103 bulk a	89.3	1.98	8.60	0.14
B8103 bulk b	86.4	1.99	11.0	0.59
B8103 Cu-Sn matrix	95.7	2.35	1.94	0.00
B8103 Pb globule	10.1	0.00	79.8	10.2
B8764 bulk a	70.0	1.42	24.02	4.56
B8764 bulk b	68.4	3.30	24.72	3.63
B8764 Pb globule a	16.1	0.40	68.95	14.52
B8764 Pb globule b	26.2	0.60	52.26	21.0
B8764 Cu-Sn matrix	75.4	3.50	17.3	3.83
B9803 bulk a	72.7	1.76	25.0	0.36
B9803 bulk b	85.1	1.93	12.6	0.39
B9803 Pb globule a	2.75	0.00	97.3	0.00
B9803 Pb globule b	1.00	0.00	99.0	0.00
B9803 Cu-Sn matrix	96.0	2.37	1.65	0.00

Most minerals identified in the micromorphological study of the thin sections have their origins in igneous or metamorphic rocks. Furthermore, the micromorphological study provides a description of the soil components that corresponds with the results from the pXRF and XRD analyses.

5. CONCLUSIONS

The overarching purpose of this research was to obtain a better understanding of the various factors influencing the degradation of a set of Roman artefacts coming from Rakafot 54 in Israel, by using a multi-analytical approach that relied on elemental and mineralogical characterisation, as well as microscopy. The first objective was to identify the main alloy components. This was accomplished by carrying out a preliminary pXRF screening on the artefact surfaces before cleaning, which showed that the alloys were all copper-lead-tin based. The second goal of this research was the determination of possible corrosion products of the objects, which was done by carrying out XRD analysis on small corrosion powder samples. The results here indicate a strong presence of copper hydroxy-chlorides such as atacamite and clinoatacamite. Paratacamite was also detected in the majority of the samples and finds partial confirmation in the detection of small amounts of Zn with pXRF. Additionally, some lead sulphates were detected, which could be correlated with the elemental data.

Finally, the main soil components were identified. By combining pXRF, XRD, and micromorphology, it was shown that the soil mainly consists of quartz, calcite, feldspars, clay minerals, and gypsum. The SEM-EDS results indicate a general presence of Pb globules in most samples, with a surrounding matrix of Cu-Sn.

Although the micromorphological study indicates local differences in soil components of the various samples, often related to burning and organic materials (presence of phytoliths and spherulites), these differences do not appear to have a clear effect on the corrosion products. The differences in intensities of the diffraction peaks representing the various corrosion products, and the absence of cuprite in one sample could be related to inconsistencies in sampling depth and small sample size. Additionally, it is possible that some soil features, such as the presence of chlorides, negate the effect that small variations in soil and alloy components could have. While there are several limitations to this research, mostly resulting from the relatively small amounts of corrosion available for analysis, the presented results provide a first insight into the corrosion processes at the site, and interesting directions for future research.

AUTHOR CONTRIBUTION

Manuel J.H. Peters: Conceptualisation, Methodology, Software, Formal analysis, Investigation, Data Curation, Writing - Original Draft, Visualisation.

Yuval Goren: Formal analysis, Resources, Data Curation, Writing - Original Draft, Supervision, Funding acquisition.

Peter Fabian: Resources, Data Curation.

José Mirão: Resources, Supervision, Funding acquisition.

Carlo Bottaini: Resources, Supervision.

Sabrina Grassini: Validation, Supervision.

Emma Angelini: Validation, Supervision, Project administration, Resources, Funding acquisition.

ACKNOWLEDGEMENT

The authors would like to thank Roxana Golan for her work with the SEM, and Mafalda Costa and Dulce Valdez for their assistance in the interpretation of the diffractograms. The research presented in this paper was part of a doctoral dissertation [12], carried out mainly using data collected at Politecnico di Torino, Ben-Gurion University of the Negev, and Universidade de Évora, as part of H2020-MSCA-ITN-2017, ED-ARCHMAT (ESR7). This project has received funding from the European Union's Horizon 2020 research and innovation programme under the Marie Skłodowska-Curie grant agreement No 766311.

REFERENCES

[1] H. Eshel, The Bar Kochba revolt, 132-135. In W. D. Davies, L. Finkelstein, S. T. Katz (Eds.), The Cambridge History of Judaism (2006) (pp. 105–127). ISBN 978-0-521-88904-9.

[2] A. Sneh, M. Rosensaft, Geological Map of Israel 1:50,000, Sheet 14-1: Netivot, Jerusalem, 2008.

[3] O. Crouvi, R. Amit, M. Ben Israel, Y. Enzel, Loess in the Negev Desert: Sources, Loessial Soils, Palaeosols, and Palaeoclimatic Implications, in Y.Enzel, O.Bar-Yosef (eds), Quaternary of the Levant, Environments, Climate Change, and Humans, Cambridge, UK, 2017, pp.471-482.
DOI: 10.1017/9781316106754.053

[4] E. Angelini, F. Rosalbino, S. Grassini, G. M. Ingo, T. De Caro, Simulation of corrosion processes of buried archaeological bronze artefacts, in P. Dillmann, G. Béranger, P. Piccardo, H. Matthiesen (eds), Corrosion of Metallic Heritage Artefacts: Investigation, Conservation and Prediction for Long-Term Behaviour, European Federation of Corrosion Publication 48, Woodhead Publishing, Cambridge, UK, 2007, pp. 203–218, ISBN: 978-1-845-69301-5

[5] Y. Goren, I. Finkelstein, N. Na'aman, Inscribed in Clay: Provenance Study of the Amarna Tablets and Other Ancient Near

Eastern Texts, Tel Aviv. 2004, pp. 112-113 with references, ISBN: 965-266-020-5.

[6] A. G. Nord, E. Mattson, K. Tronner, Factors Influencing the Long-Term Behavior of Bronze Artefacts in Soil, Protection of Metals, vol.41, 2005, pp.339-346.
DOI: 10.1007/s11124-005-0045-9
R. Frost, Raman Spectroscopy of Selected Copper Minerals of Significance in Corrosion, Spectrochimica acta. Part A, Molecular and biomolecular spectroscopy, vol. 59, 2003, pp. 1195-1204.
DOI: 10.1016/S1386-1425(02)00315-3

[7] R. Fernandes, B. J. H.van Os, H. D. J. Huisman, The use of Hand-Held XRF for investigating the composition and corrosion of Roman copper-alloyed artefacts, Heritage Science, vol. 1, 2013.
DOI: 10.1186/2050-7445-1-30

[8] O. Oudbashi, Multianalytical study of corrosion layers in some archaeological copper alloy artefacts, Surface and Interface Analysis, vol. 47, 2015, pp. 1133-1147.
DOI: 10.1002/sia.5865

[9] P. Piccardo, B. Mille, L. Robbiola, Tin and copper oxides in corroded archaeological bronzes, in P.Dillmann, G.Béranger, P. Piccardo, H. Matthiesen (eds), Corrosion of Metallic Heritage Artefacts: Investigation, Conservation and Prediction for Long-Term Behaviour, European Federation of Corrosion Publication 48, Woodhead Publishing, Cambridge, UK, 2007, pp. 239–262.
ISBN: 978-1-845-69301-5.

[10] L. Robbiola, J. M. Blengino, C. Fiaud, Morphology and Mechanisms of Formation of Natural Patinas on Archaeological Cu-Sn Alloys, Corrosion Science, vol. 40, 1998, pp. 2083-2111.
DOI: 10.1016/S0010-938X(98)00096-1

[11] M. J. H. Peters, Innovative techniques for the assessment of the degradation state of metallic artefacts, PhD thesis, Turin: Politecnico di Torino, 2021.